DOI: 10.1002/ejic.200900103

A-Frame-Containing Organometallic Oligomers Constructed From Homo- and Heterobimetallic M(μ-dppm)$_2$M′ (M/M′ = Pd, Pt) Building Blocks

Sébastien Clément,[a] Shawkat M. Aly,[a] Jérôme Husson,[b] Daniel Fortin,[a] Carsten Strohmann,[c] Michael Knorr,*[b] Laurent Guyard,[b] Alaa S. Abd-El-Aziz,[d] and Pierre D. Harvey*[a]

Keywords: Platinum / Palladium / Polymers / Isocyanide ligands / Luminescence

The homo- and heterodinuclear complexes XM(μ-dppm)$_2$-M′X (M = M′ = Pd, X = Cl **1a**; M = M′ = Pd, X = I **1b**; M = Pd, M′ = Pt, X = Cl **2a**; M = Pd, M′ = Pt, X = I **2b**; M = M′ = Pt, X = Cl **3a**; M = M′ = Pt, X = I **3b**) react with the diisocyanide ligand 1,2-bis(2-isocyanophenoxy)ethane (diNC) or the more soluble 1,2-bis(2-isocyano-4-*tert*-butylphenoxy)ethane (*t*BudiNC) in a 1:1 ratio to provide the thermally stable polymeric materials **4**–**9** {[XM(μ-dppm)$_2$M′(μ-CN-C$_6$H$_3$R-2-OCH$_2$-CH$_2$O-2-C$_6$H$_3$R-NC)]X}$_n$ (M = M′ = Pd, R = H, X = Cl **4a**, I **4b**; R = *t*Bu, X = Cl **7**; M = M′ = Pt, R = H, X = Cl **5a**, I **5b**; R = *t*Bu, X = Cl **8**; M = Pd, M′ = Pt, R = H, X = Cl **6a**, I **6b**; R = *t*Bu, X = Cl **9**). These A-frame-containing materials have been characterized in solution or in the solid state by ^{31}P NMR (MAS) spectroscopy, elemental analysis, MALDI-TOF, DSC, TGA, IR and T_1/NOE [^{31}P NMR spin-lattice relaxation time and nuclear Overhauser enhancement constant (NOE) measurements]. The IR, Raman [ν(CN) bridging vs. terminal] and NMR spectroscopic data reveal the presence of an A-frame structure for these new materials. Evidence of an oligomer (including at least two units, determined by T_1/NOE experiments) – polymer equilibrium in solution was obtained at room temperature. These polymers are luminescent (phosphorescence) at 77 K in solution and in the solid state, exhibiting broad emission bands in the 500–800 nm range.

Introduction

Metal-containing macromolecules and coordination and organometallic polymers have been the subject of growing interest during the past few years.[1,2] These materials take on a multitude of design concepts and their applications are as varied as their structures. The choice of appropriate metallic centers, ligands, and substituents offers the possibility to tune the chemical, optical, physical, and electrical properties of the resulting materials. As a result, organometallic polymers containing a metal–ligand bond in the main chain have been extensively studied, especially rigid-rod polymers connected by linear π-conjugated organic linkers such as diacetylide and diisocyanide.[3] In general, the electronic structure of isocyanides is similar to that of CO, although isocyanides are considered to be stronger σ-donor and weaker π-acceptor ligands than CO. However, their σ-donor/π-acceptor propensities can be fine-tuned by varying the nature of the substituent R on isocyanides CNR.[4] Like CO, metal-containing isocyanide ligands may adopt different bonding modes (terminal, semi-bridging, and symmetric μ$_2$-bridging coordination; Scheme 1).[4b,5] Due to this versatility in bonding modes with metal complexes and their ability to give rise to complexes with unusual properties,[6] isocyanide ligands are of special interest for the design of new photonic materials with defined properties.

In this context, one of us has recently investigated the physicochemical properties of unconjugated and conjugated dppm-bridged (dppm = Ph$_2$PCH$_2$PPh$_2$) homo- and heterobimetallic polymers containing functionalized diisocyanide ligands in detail (Scheme 2) and demonstrated their potential applications in photonics.[3f,7a,7b] Among the unconjugated materials, our groups have also recently reported the first example of an A-frame-containing organometallic polymer, namely {[{ClPd(μ-dppm)$_2$Pt(μ-CN-C$_6$H$_4$-2-OCH$_2$CH$_2$O-2-C$_6$H$_4$-NC)}Cl]$_n$} (**5a**), built from the heterobimetallic fragment Pd(μ-dppm)$_2$Pt (Scheme 2).[7c] The site

[a] Département de Chimie, Université de Sherbrooke, 2550 Boul. Université, Sherbrooke, PQ, Canada, J1K 2R1, Canada
Tel.: +1-819-821-7092
Fax: +1-819-821-8017
E-mail: Pierre.Harvey@USherbrooke.ca
[b] Institut UTINAM UMR CNRS 6213, Université de Franche-Comté, Faculté des Sciences et des Techniques, La Bouloie, 16 Route de Gray, 25030 Besançon, France
Tel.: +33-3-81666270
Fax: +33-3-81666438
E-mail: michael.knorr@univ-fcomte.fr
[c] Technische Universität Dortmund, Anorganische Chemie, Otto-Hahn-Str. 6, 44227 Dortmund, Germany
[d] University of British Columbia, Okanagan, 3333 University Way, Kelowna, British Columbia, Canada, V1V 1V7
Supporting information for this article is available on the WWW under http://www.eurjic.org or from the author.

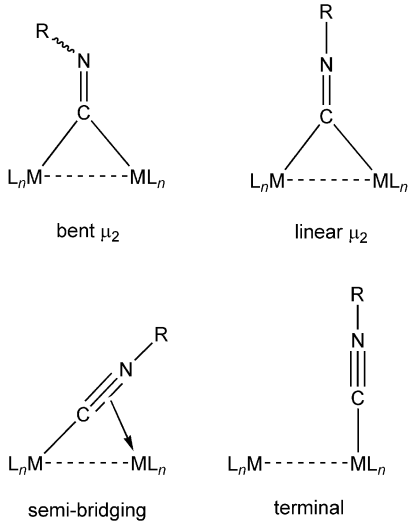

Scheme 1.

selectivity around the Pt center and the luminescence properties of this new polymer appear promising for elaborating "head-to-tail" polymers by making a judicious choice of mixed-donor bidentate ligands (i.e. phosphane and isocyanide). An extension of our studies to the homodinuclear analogs as well as the investigation of the counterion in this class of materials now appears to be required for a more comprehensive understanding of which parameters could lead to a selective tuning of the physicochemical properties of the resulting materials. The structural, physical, and photophysical properties of these new polymers are reported in detail herein.

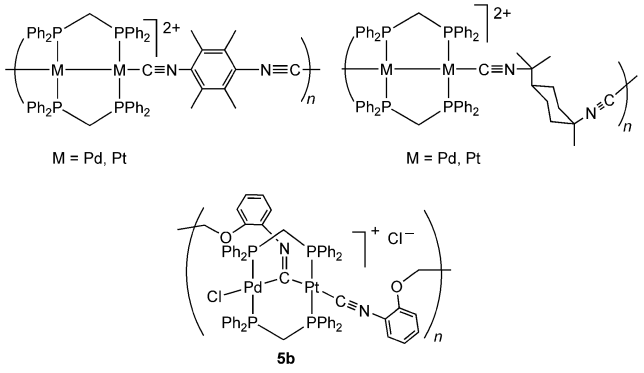

Scheme 2.

Results and Discussion

Polymer Synthesis and Characterization

The conclusion of our previous work[7c] on the unconjugated A-frame-containing heterobimetallic polymer **5a** urged us to introduce a systematic variation of the nature of the metal centers, the halide ligands, and the alkyl group (*t*Bu) on the diisocyanide ligand so as to elucidate which of these factors controls the physicochemical properties of this kind of material. The introduction of a *t*Bu group was undertaken in order to increase the solubility of the resulting materials and thereby facilitate their characterization in solution. The crystal structure of *t*BudiNC[8] is depicted in Figure 1. The structure exhibits a conformation where the two bulky *tert*-butyl groups are placed far from each other, thereby reducing the steric interactions between them. This particular conformer has the two isocyanide donors pointing towards the same face, very likely due to crystal packing. The polymer formation discussed below will provide evidence for the presence of other conformations of the isocyanide groups.

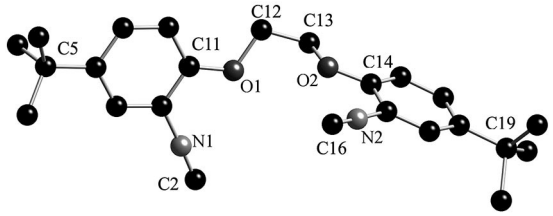

Figure 1. Ball-and-stick representation of *t*BudiNC with the numbering scheme. H-atoms have been omitted for clarity. Selected bond lengths [Å] and angles [°]: C(1)–N(1) 1.398(3), C(15)–N(2) 1.393(3), C(2)–N(1) 1.162(4), C(16)–N(2) 1.150(4), C(11)–O(1) 1.355(3), C(12)–C(13) 1.476(4), C(12)–O(1) 1.437(3), C(4)–C(5) 1.518(4), C(5)–C(6) 1.525(4), C(5)–C(7) 1.537(4); C(1)–N(1)–C(2) 177.3(3), C(15)–N(2)–C(16) 178.2(3), C(4)–C(5)–C(6) 111.9(2), C(4)–C(5)–C(7) 108.1(2), C(13)–C(12)–O(1) 108.4(2), C(11)–O(1)–C(12) 117.4(2).

The A-frame polymers were synthesized by direct reaction of the homo- or heterobimetallic complexes **1**–**3** with diNC or *t*BudiNC in a 1:1 ratio (Scheme 3).

The resulting orange diNC-containing materials **4**–**6** are very sparingly soluble and readily precipitate. This low solubility contrasts with polymers **7**–**9**, which contain diisocyanide ligands bearing a solubilizing group (*t*Bu). Evidence for the A-frame geometry in these polymers was obtained from the presence of two distinct absorptions at around 1630 and 2170 cm^{-1} for the bridging and terminal isocyanides, respectively. The vibrational ν(N≡C) (1619 and 1623 cm^{-1} for **4a** and **4b**, respectively) and the ν(N=C) solid-state Raman scatterings (2164 and 2171 cm^{-1} for **4a** and **4b**, respectively) also support this A-frame structure. Due to their low solubility, characterization of polymers **4**–**6** was performed by ^{1}H and ^{31}P{^{1}H} solid-state MAS-NMR spectroscopy or in solution with [D$_6$]DMSO as solvent when possible. The ^{31}P NMR spectra of these polymers should exhibit two characteristic resonances attributable to the two different phosphorus sites. However, in most cases the resonances for these materials are broad and ill-defined, thus making their analysis difficult. This observation strongly suggests that these insoluble (or weakly soluble) materials are polymers rather than oligomers in the solid state.

The introduction of an alkyl side-chain (*t*Bu) on the aryl diisocyanide renders the polymers **7**–**9** slightly more soluble, thus allowing their characterization by ^{1}H, ^{13}C, and ^{31}P NMR spectroscopy in solution. Their IR spectra also exhibit two absorptions in the ν(N≡C) region, thus confirming

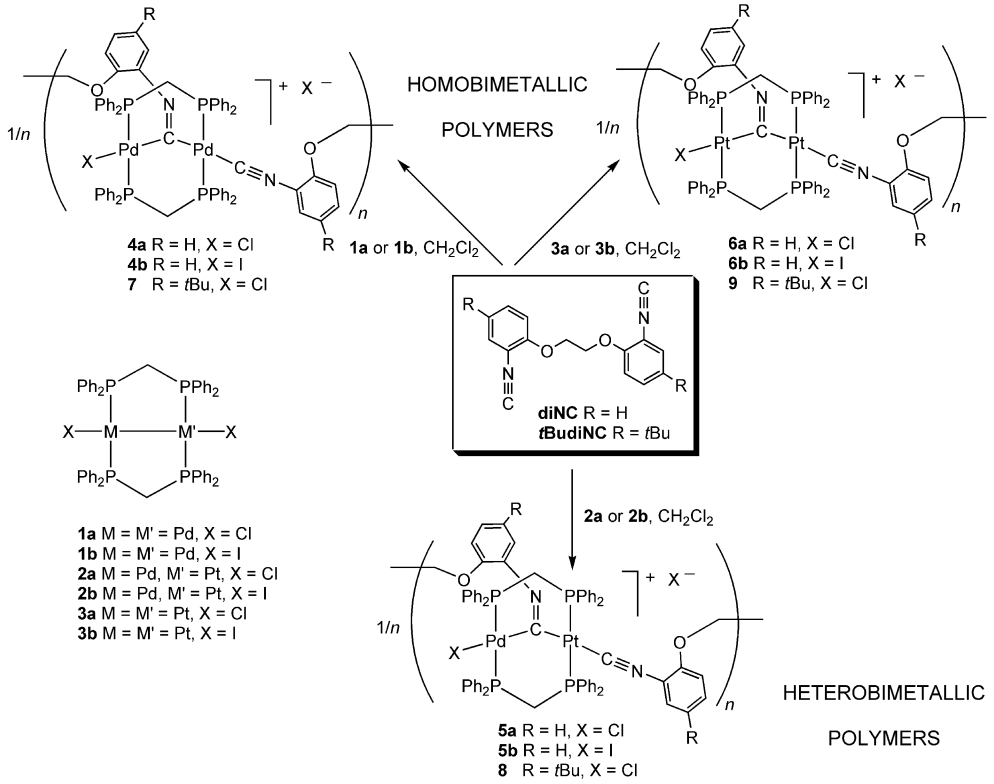

Scheme 3.

the expected presence of the terminal and bridging groups (see Experimental Section). The presence of the *t*Bu group in these polymers is evident from the characteristic singlet in the range δ = 1–1.5 ppm in the ^{1}H NMR spectra and the two expected ^{13}C resonances in the range δ = 0–30 ppm. The homobimetallic Pd-containing polymer **7** exhibits a multiplet centered at δ = 17 ppm in its ^{31}P{^{1}H} NMR spectrum. This value compares favorably to the chemical shift of the sharp singlet obtained for the model compound [ClPd(μ-dppm)$_2$(μ-C=N-C$_6$H$_4$-4-*i*Pr)PdCl] (**10**) used in this work for T_1/NOE experiments (see below). The A-frame structure of this model compound was confirmed by X-ray diffraction (Figure 2). The structure exhibits the typical A-frame structure where the CNR group bridges the two Pd atoms symmetrically and does not occupy the axial position. The bond lengths are normal and similar to those in [ClPd(μ-dppm)$_2$(μ-C=N-C$_6$H$_5$)PdCl].[9] The Pd···Pd distance of 3.188(4) Å found in the latter compound is comparable to the distance of 3.1943(17) Å in **10**.

The ^{31}P NMR spectrum of the heterobimetallic polymer **8** is characterized by two sets of AA′XX′ resonances attributable to ^{31}P–Pt (δ = 16.4 ppm) and ^{31}P–Pd (δ = 18.7 ppm). The former resonance is flanked by the two expected ^{195}Pt satellites ($^1J_{Pt,P}$ = 2690 Hz). In comparison with the ^{31}P NMR spectroscopic data of the structurally characterized model compound [IPd(μ-dppm)$_2$(μ-C=N-C$_6$H$_4$-2-OCH$_3$)-Pt(CN-C$_6$H$_4$-2-OCH$_3$)]I (**11**), which has been reported elsewhere ($\delta_{Pt\text{-bound P}}$ = 16.1, $\delta_{Pd\text{-bound P}}$ = 18.3 ppm; $^1J_{Pt,P}$ = 3210 Hz),[10b] these latter values compare favorably with those for other A-frame complexes, thereby illustrating the

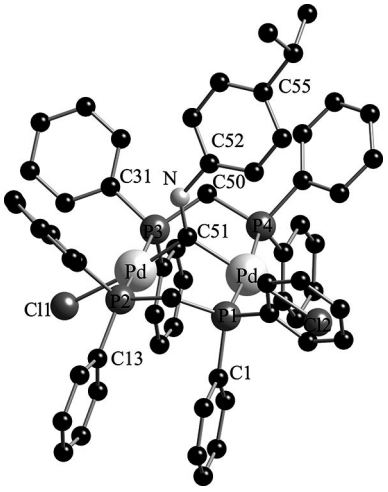

Figure 2. Ball-and-stick representation of **10** with numbering scheme. H-atoms have been omitted for clarity. Selected bond lengths [Å] and angles [°]: Pd(1)–C(51) 2.007(14), Pd(1)–P(1) 2.313(5), Pd(2)–C(51) 1.933(16), Pd(1)–P(4) 2.336(5), C(51)–N(1) 1.23(2), Pd(2)–P(2) 2.318(5), Pd(1)–Cl(1) 2.435(4), Pd(2)–P(3) 2.349(5), Pd···Pd 3.1943(17), C(52)–N(1) 1.42(2); Cl(1)–Pd(1)–C(51) 178.9(4), Cl(2)–Pd(2)–C(51) 173.7(5), P(2)–Pd(2)–C(51) 85.5(5), P(1)–Pd(1)–C(51) 87.2(5), P(3)–Pd(2)–C(51) 86.2(5), P(4)–Pd(1)–C(51) 90.4(12), P(2)–Pd(2)–P(3) 169.9(2), P(4)–Pd(1)–Cl(1) 94.74(15), P(1)–Pd(1)–P(4) 173.17(16), P(3)–Pd(2)–Cl(2) 93.25(19), Pd(1)–C(51)–Pd(2) 108.4(9), Pd(1)–C(51)–N(1) 132.6(12), C(51)–N(1)–C(52) 133.0(15), Pd(2)–C(51)–N(1) 118.8(11), P(2)–C(49)–P(1) 114.2(10), P(3)–C(50)–P(4) 114.0(7).

site selectivity of substitution of the halide ligand by the CNR group at the Pt metal. This preference for the plati-

num site in substitution reactions was noticed previously by us from the reactivity of the heterobimetallic complex **1a** towards isocyanides, phosphanes, and hydrides.[10]

Properties of the Polymer in the Solid State

The thermal stability of the materials was analyzed by TGA (see Figure 3 and Supporting Information).

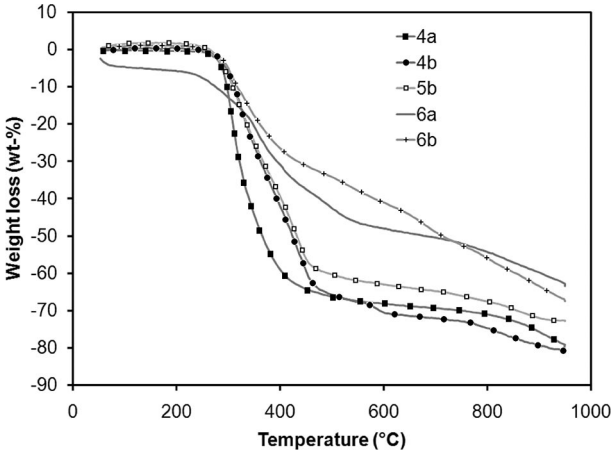

Figure 3. TGA traces for the A-frame-containing polymers **4a**,**b**, **5b**, and **6a**,**b**. The ATG trace for **5a** is available in ref. [7c].

These materials exhibit good thermal stability under Ar. The first weight losses upon heating occur at temperatures exceeding 210 °C for **6a**, 230 °C for **5b**, **6b**, **7**, and **8**, 250 °C for Pd polymers **9**, and 290 °C for **5a** (see Figure 4 and Supporting Information). The weight loss vs. temperature plots exhibit, in general, plateaus around 700–800 °C. Based on previous studies of the thermal stability of coordination/organometallic polymers using $[RNC\text{-}M(\mu\text{-dppm})_2M\text{-}CNR]^{2+}$ building blocks (M = Pd, Pt),[7a] it is assumed that the loss or decomposition of diisocyanide occurs at lower temperatures than that of the more robust $M(\mu\text{-dppm})_2\text{-}M'^{2+}$ fragments (see Supporting Information). In fact, loss of the phenyl groups (dppm) must occur to account for the weight losses at higher temperatures. Proposed TGA weight-loss assignments for all these metallopolymers are presented in the Supporting Information.

Not surprisingly, the DSC traces indicate no glass transition for A-frame polymers **4**–**9** between –30 °C and the decomposition temperature. Decomposition of all these metallopolymers produces an insoluble black material whose exact nature remains to be elucidated. The lack of a glass transition may be associated with the limited motion of the polymer chain due to the size of the $[M(\mu\text{-dppm})_2\text{-}M]^{2+}$ fragment and/or the relative rigidity of the chain due to internal steric hindrance between the diNC and *t*BudiNC ligands. This behavior is in good agreement with the previously more "flexible" binuclear $[Pd(\mu\text{-dppm})_2Pd]^{2+}$-containing polymers containing dmb (dmb = 1,8-diisocyano-*p*-menthane) and diphosphane ligands and for the homodinuclear $M(\mu\text{-dppm})_2M$ (M = Pd, Pt) complexes containing diisocyanide building blocks.[7b,11]

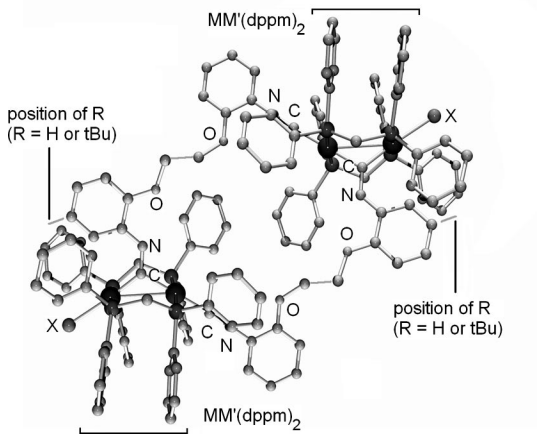

Figure 4. Qualitative computer modeling of the dimers [using PC-Model (version 7.0)] illustrating the possible close contacts, especially Ph···Ph, *t*Bu···Ph, and *t*Bu···X contacts, in the dimer in solution.

Properties in Solution

Our attempts to dissolve a maximum amount of the very weakly soluble materials **4**–**6** involved the use of an ultrasound bath. The resulting suspension was filtered in order to obtain a clear solution. However, a precipitate formed at the bottom of the flask after several hours. This precipitate could be redissolved using the same procedure, and the process is cyclic and reproducible. In order to explain this phenomenon, a polymer(solid)-oligomer(solution) equilibrium was strongly suspected. A similar behavior has been described previously by our group for the binuclear complexes $[ClPd(dmb)_2PdCl]$[7b] and other d^8 Pd(diphos)(isocyanide)-containing polymers [diphos = $Ph_2P\text{-}(CH_2)_m\text{-}PPh_2$; m = 2–6].[11] Interestingly, this latter work[11] clearly demonstrated from X-ray crystallographic studies that the most common oligomer is the dimer. Attempts to estimate the M_n values by MALDI-TOF spectrometry proved inconclusive since only the fragments $M(\mu\text{-dppm})_2M'$ and $XM(\mu\text{-dppm})_2M'$ (X = Cl, I, M = Pd, Pt and M′ = Pd, Pt) were observed (see the Supporting Information for a typical example). This result indicates the fragility of this kind of polymer under MALDI-TOF conditions.[11] Consequently, the M_n values in solution were estimated by the T_1/NOE method, which is fully explained elsewhere.[12] Only a brief description is provided here. This NMR method offers the possibility of long data acquisition times in the case of solubility problems, as is the case here. The molecular dimension can be estimated from the Stokes-Einstein-Debye equation, assuming a spherical shape, if the correlation time, τ_c, is known ($\tau_c = V\eta_{visc}/kT$; η_{visc} = solvent viscosity; k = Boltzmann constant; T = temperature). In order to measure τ_c, one must know the spin-lattice relaxation time related to dipole-dipole interactions, T_1^{DD}, which is given by Equation (1).

$$1/T_1^{DD} = \Sigma\ (\hbar^2\gamma^2_P\gamma^2_H/4\pi^4 r^6_{PH})\ \tau_c \quad (1)$$

In the extreme narrowing limit,[13] where ħ is the Planck constant, γ is the gyromagnetic ratio for the interacting nu-

clei (^{31}P and ^{1}H in this case),[14] and r is the distance between the probe (here at 121.4 MHz ^{31}P) and the nearest interacting nuclei (here ^{1}H). The T_1^{DD} data (here at 300 MHz ^{1}H) can be extracted from experimental T_1 and NOE measurements[14b] according to Equation (2).

$$1/T_1^{DD} = \eta/(\eta_{max}\ T_1) \quad (2)$$

where η is the fractional NOE constant, η_{max} the maximum η value in the extreme narrowing limit (here $\eta_{max} = \gamma_H/2\gamma_P$), and T_1 is the experimental spin-lattice relaxation time. Examples of T_1 recovery traces for the model compound **10** and polymer **11** are presented in the Supporting Information. The strategy involves comparing the hydrodynamic volume of a known compound (ideally characterized crystallographically) with that of the unknown ones. One parameter that must be taken into account is that the standard molecule must be closely related to the sample molecule. In this work, the probe nuclei are the ^{31}P atoms because of their strong signal. Combining Equations (1) and (2) with the Stokes–Einstein–Debye equation gives Equation (3) where "sam" and "sta" stand for sample and standard, respectively.

$$\frac{T_1(\text{sam})}{T_1(\text{sta})} = \frac{\eta_{PH}(\text{sam})}{\eta_{PH}(\text{sta})} \cdot \frac{V(\text{sta})}{V(\text{sam})} \cdot \frac{\Sigma[1/r^6_{PH}(\text{sta})]}{\Sigma[1/r^6_{PH}(\text{sam})]} \quad (3)$$

This equation requires a knowledge of the interatomic distances between the ^{31}P probe nucleus and the surrounding ^{1}H nuclei. Due to the structural similarity between the bimetallics polymers **4**–**6** and polymers **7**–**9**, we assumed that no significant difference would be obtained for the T_1/NOE experiment for these metallopolymers containing diNC or *t*BudiNC. Consequently, just one polymer in every series (diNC, polymer **5a** and *t*BudiNC, polymer **7**) was investigated. The model compounds [ClPd(μ-dppm)$_2$(μ-C=N-C$_6$H$_4$-4-*i*Pr)PdCl] (**10**), where the bridging isocyanide bears an alkyl group (*i*Pr), and [ClPd(μ-dppm)$_2$(μ-C=N-C$_6$H$_4$-2-OCH$_3$)Pt(CN-C$_6$H$_4$-2-OCH$_3$)]Cl (**11**), described elsewhere,[10b] which exhibit very close structural similarities to **5a**, were chosen as standard molecules for the metallopolymers **7** and **5a**, respectively. The largest magnetic interactions between the P and H atoms in model compound **11** are the P···H$_2$C and P···H(*ortho*-Ph) interactions within the dppm ligand. These interactions exhibit the shortest distances based on average values extracted from the X-ray structure[5] and computer modeling (Scheme 4). The same situation occurs for compound **10**, therefore the distances presented in Scheme 4 are the same.

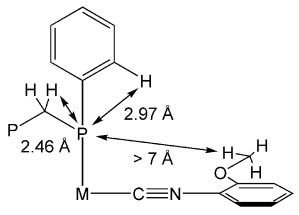

Scheme 4.

Because the chemical environment around the P atom is about the same for the sample and standard **11** (in **10**), the η constants are about the same as well. This means that the terms $[\Sigma\ 1/r^6_{PH}(\text{sam})]/[\Sigma\ 1/r^6_{PH}(\text{sta})]$ and $\eta_{PH}(\text{sam})/\eta_{PH}(\text{sta})$ are approximately unity and the V(sta)/V(sam) ratio is given by the T_1(sam)/T_1(sta) ratio. Since V(sam) is not known from crystallography, one can use computer modeling. By computing the gas-phase volumes of the standard and sample as a monomer, the oligomer size n (number of repetitive units), can be calculated; see Equation (4).

$$n = [V(\text{sam})_{exp}/V(\text{sta})_{exp}]\cdot[V(\text{sta})_{cald.}/V(\text{sam})_{cald}] \quad (4)$$

The T_1 data for **5a** (standard for polymer **11**) and **11**, and for **10** (standard for polymer **7**) and **7** are listed in Table 1. All experiments were performed in CD_2Cl_2, a non-coordinating solvent, to avoid the breakdown of the polymer due to a solvent donor molecule.

Table 1. T_1, V (for one unit) and calculated n for **5a**, **7**, **10**, and **11**.

Compound or polymer	T_1 [s]	Gas phase V for one unit [Å^3]	n (±10%)
5a	1.99	1319	–
7	1.56	1493	≈1.5
10	2.93	1226	–
11	1.07	1311	≈1.9

The T_1 values for polymer **11** and standard **5a** are 1.07 and 1.99 s, respectively, which means that $[V(\text{sam})_{exp}/V(\text{sta})_{exp}]$ is 1.9. With $V(\text{sta})_{cald.}/V(\text{sam})_{cald}$ [1319/1311 (for one unit), obtained from the calculations], n is $1.9 \times 1.00 = 1.9$ (i.e. about 2). Metallopolymer **5a** can therefore only be a small oligomer (i.e. most likely a dimer) and not much larger in solution, which is completely consistent with the observed solubility.

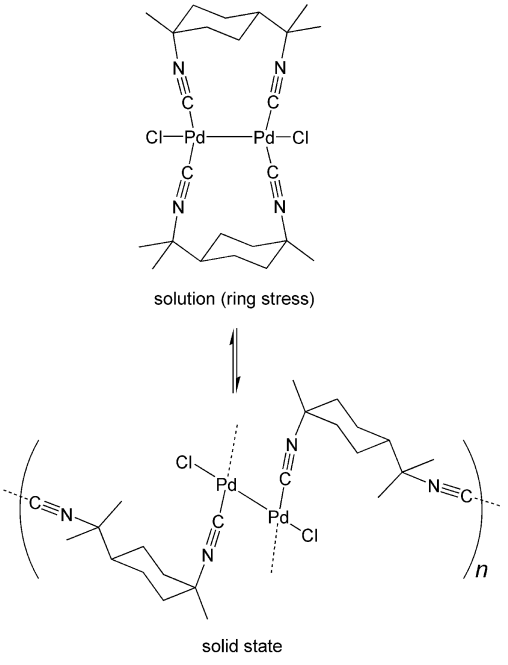

Scheme 5.

A similar analysis for metallopolymer **7** and model compound **10** gave a value of *n* of about 1.5 (due to a large uncertainty in the method), which is ambiguous. However, we conclude that *n* must be equal to 2. The oligomer (including monomer) in solution/polymer in the solid state equilibrium is well established, notably for the Pd_2-bonded species $Pd_2(dmb)_2Cl_2$ (Scheme 5).[7b]

A similar situation may be occurring here, with internal steric hindrance driving the ring-opening polymerization. This proposal is supported by simple qualitative computer modeling (PC-Model) of such a dimer, where some inner phenyl groups may be in close contact and the *t*Bu groups may interact with neighboring phenyl and halide groups (Figure 4).

Electronic Spectra and Photophysics

Absorption Spectra

The absorption spectra of these polymers exhibit two low energy bands in the 350–450 nm range (see the Experimental Section). Reliable extinction coefficients for these bands could not be obtained owing to the limited solubility of our polymers. The band position and band-shape observed for these materials compare very favorably with other d^8-d^8 A-frame systems based on iridium, palladium, and platinum metal centers, thus corroborating the A-frame environment about the metal atoms.[7c,9,15] A detailed investigation of the corresponding model compounds at the DFT and TDDFT levels of theory indicates that the lowest energy band in the 420–465 nm range is a M/XLCT (metal/halide-to-isocyanide charge-transfer) band.[10b]

Luminescence Properties of tBudiNC

For assignment purposes, the uncoordinated *t*BudiNC ligand was investigated in the solid state. This compound exhibits a maximum emission band at 400 nm and the excitation spectrum reveals a maximum at 330 nm (see the Supporting Information). The small Stokes shift between these two bands suggests that this emission is fluorescence, most likely arising from a ππ* excited state. This assessment is important because the presence of such emissions in A-frame-containing species is easily addressable. No lower energy emissions from this ligand were observed, although this may be possible in the presence of heavy metals (heavy metal effect).[16]

Luminescence and Photophysical Properties of the A-frame Species

None of the investigated polymers (and short oligomers in solution) listed in Table 2 are luminescent either in solution or in the solid state at room temperature, except for **4b**, which is weakly luminescent at 298 K in the solid state. This property may be associated with an energy wasting photoinduced M(μ-isocyanide)M bond scission or ligand dissociation in the excited states. However, the compounds become luminescent at 77 K in PrCN (Table 2, Figures 5 and 6) and in the solid state (see the Supporting Information), most likely because the photodissociation processes are dramatically slowed down in the solid state at low temperature. Note that model compound **10** is not luminescent at either room temperature or at 77 K.

Table 2. Photophysical data for polymers **4**–**9** in PrCN at 77 K.

	PrCN			Solid
	λ_{em} [nm]	τ_e [μs]	ϕ_e	λ_{em} [nm]
4a	680	0.20 ± 0.01	0.0048	725
4b	705	0.19 ± 0.01	0.0028	740
5a	660	0.18 ± 0.01	0.0056	703
5b	730	0.78 ± 0.01	0.0048	735
6a	615	1.78 ± 0.01	0.003	635
6b	630	2.12 ± 0.09	0.002	715
8	705	2.87 ± 0.06	0.004	735
9	615	5.56 ± 0.09	0.004	640

Unstructured emission bands are observed in the 500–800 nm range and the excitation spectra can be well superimposed on the absorption ones, thus indicating that the absorbing and emitting species are the same (Figure 5). Some slight differences are noted in this comparison because competitive upper-excited state non-radiative processes may be taking place (see, for example, **5a**), although the positions of the band maxima remain relatively the same. These latter values are in good agreement with those obtained previously by us for other homo- and heterobimetallic complexes containing a bridging isocyanide.[10b] The large Stokes shifts ($>10000\ cm^{-1}$) and lifetimes of a few microseconds suggest that the luminescence is a phosphorescence.

The maxima wavelength of these dinuclear complex-containing materials in solution or in the solid state are in the order Cl < I, thus indicating that the nature of the excited states is slightly influenced by the nature of the halide and consistent with the M/XLCT assignment.[17]

The key features of these emissions are as follows. The emission lifetimes for Pd-containing materials are shorter than those of the Pt analogues (by about one order of magnitude, Table 2). These differences in photophysical data may be assigned to a greater lability of the M–L bond in the Pd polymers in comparison with the platinum ones in the excited state, thus promoting a non-radiative deactivation pathway. In comparison with the previously reported heterobimetallic model compounds [ClPd(μ-dppm)$_2$(μ-C=N-C_6H_4-2-OCH_3)Pt(CN-C_6H_4-2-OCH_3)]Cl (**7a**; τ_e = 3.06 μs, Φ_e = 0.0079) and [ClPd(μ-dppm)$_2$(μ-C=N-C_6H_4-2-OCH_3)Pt(CN-C_6H_4-2-OCH_3)]I (**7b**; τ_e = 12.7 μs, Φ_e = 0.0043),[10b] smaller values were obtained for the heterobimetallic complex-containing polymers **5a** and **5b**. The other polymeric materials also exhibit the same features, namely short lifetimes ($0.18 < \tau_e < 0.78$ μs) and low phosphorescence quantum yields ($0.002 < \phi_e < 0.005$). This decrease in the photophysical parameters is consistent with an increase in non-radiative processes associated with supplementary vibrational modes in polymers and with deactivations promoted by intramolecular collisions.

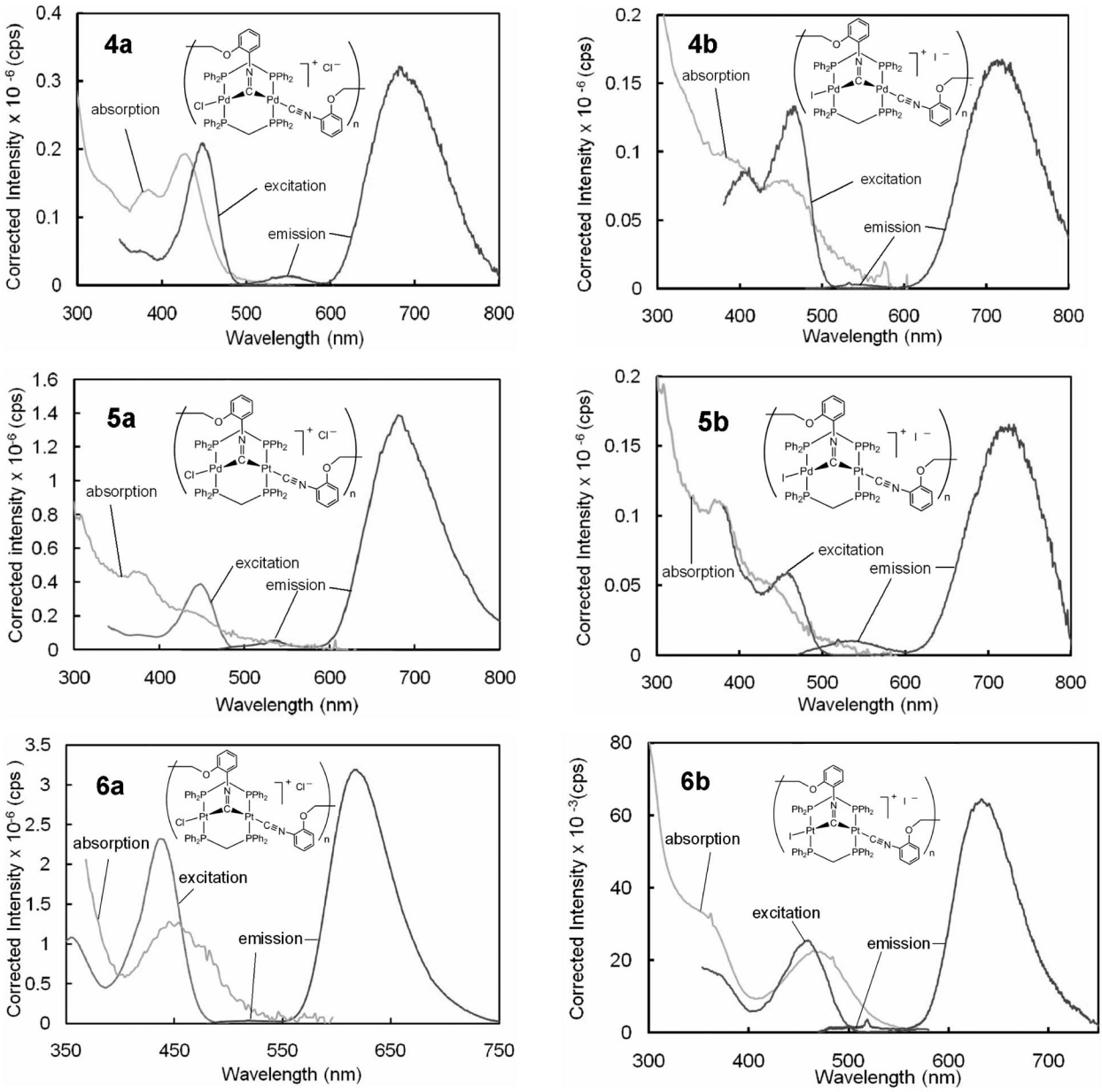

Figure 5. Absorption, emission, and excitation spectra of diNC-containing polymers **4**–**6** in PrCN at 77 K. λ_{exc} = 450 nm.

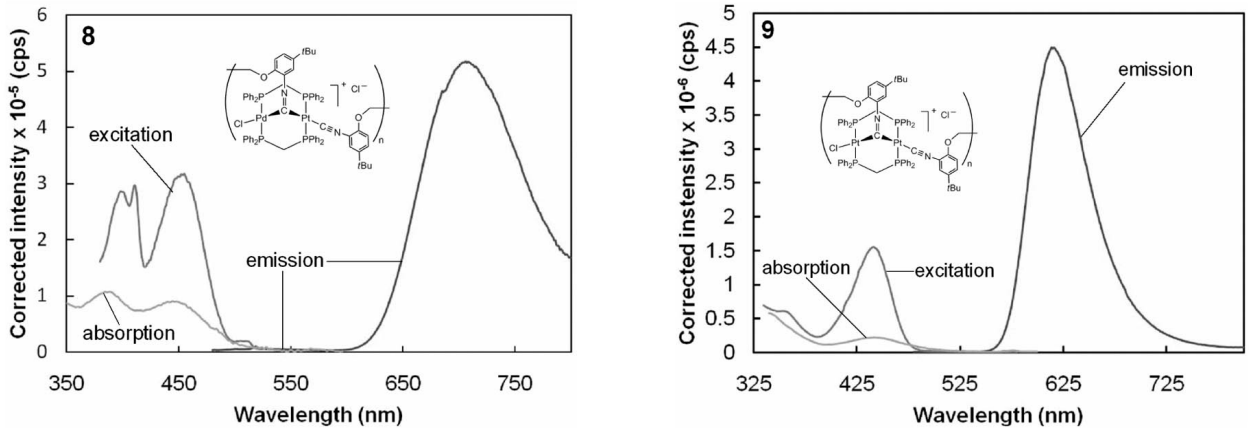

Figure 6. Absorption, emission, and excitation spectra of *t*BudiNC-containing polymers **8** and **9** in PrCN at 77 K. λ_{exc} = 450 nm.

During the course of this study, we noticed a weak emission at about 550 nm (see Figure 5 for an example). Compound **4b** was therefore investigated at different excitation wavelengths (Figure 7). Excitation at 330 nm (where the ligand absorbs) leads to the observation of two bands in the 350–600 nm window. These are easily assigned to ligand fluorescence and phosphorescence. The assignment of the second emission at 535 nm was based upon the temperature-dependent experiment (Figure 7).

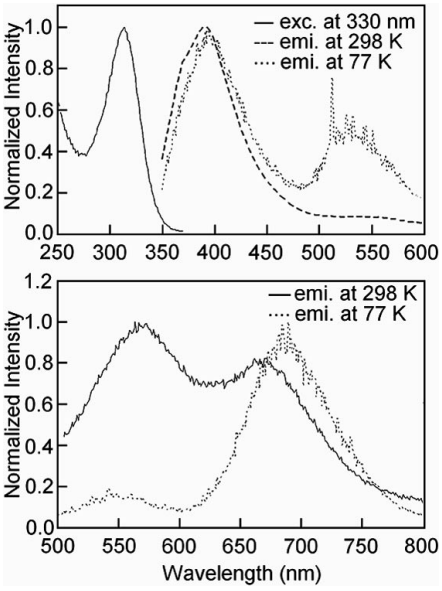

Figure 7. Top: Excitation spectrum (at λ_{em} = 390 and 556 nm) of polymer **4b** in the solid state at 298 K (−) and emission spectra of the same polymer (λ_{exc} = 330 nm) at 298 (---) and 77 K (···). Bottom: Solid-state emission spectra of polymer **4b** (λ_{exc} = 450 nm) at 298 (−) and 77 K (···).

This band is observable at both 298 and 77 K but is more intense at 77 K. The presence of ligand phosphorescence is attributed to the heavy atom effect, as anticipated. Upon excitation at 450 nm, in the lowest energy band of the compound, the luminescence of the A-frame chromophore can easily be observed, thus allowing an intensity comparison of the two bands (phosphorescence of the ligand, and emission centered on the A-frame core). The fact that ligand fluorescence and phosphorescence are still observable in polymer **4b** indicates that inefficient (i.e. slow) energy transfer from the ligand to the A-frame unit occurs. This conclusion indicates that the isocyanide bridge linking the aryl group to the inorganic A-frame residue is a modest electronic communicator, in agreement with the conclusions reached for other similar systems using [2.2]paracyclophane as the luminescent fragment.[18]

Conclusions

A series of new d^8-d^8 dinuclear A-frame polymers built upon M(μ-dppm)$_2$M′ (M = Pd, Pt and M′ = Pd, Pt) building blocks have been prepared and unambiguously characterized. The site selectivity at the Pt center for the heterobimetallic polymers has been probed and has been shown to allow further functionalization at the Pd center to build "head-to-tail" polymers by a judicious choice of mixed-donor bidentate ligands. A polymer (solid)-oligomer (solution) equilibrium has been suggested for these polymers, with the dominant species in solution being the dimer. These materials are luminescent in the solid state and in solution at 77 K. Functionalization of the diisocyanide ligands (introduction of more solubilizing side chains, *N*-protonation or -alkylation) to tune the chemical, physical, and photophysical properties of this new class of materials is in progress.

Experimental Section

Materials: All reactions were performed in Schlenk tubes under purified nitrogen. [ClPd(μ-dppm)$_2$PdCl] (**1a**), [IPd(μ-dppm)$_2$PdI] (**1b**), [ClPd(μ-dppm)$_2$PtCl] (**2a**), [IPd(μ-dppm)$_2$PtI] (**2b**), [IPt(μ-dppm)$_2$PtI] (**3b**), 1,2-bis(2-isocyanophenoxy)ethane (diNC), 1,2-bis(2-isocyano-4-*tert*-butylphenoxy)ethane (*t*BudiNC), 1-isocyano-4-isopropylbenzene, and {[ClPd(μ-dppm)$_2$Pt(μ-CN-C$_6$H$_4$-2-OCH$_2$-CH$_2$O-2-C$_6$H$_4$-NC)]Cl}$_n$ (**5a**) were prepared according to literature procedures.[7c,19–21] All solvents were dried and distilled from appropriate drying agents.

Apparatus: IR spectra were recorded with a Nicolet Nexus 470 spectrometer. All solution NMR spectra were acquired with a Bruker Avance 300 spectrometer (^{1}H: 300.13 MHz; ^{13}C: 75.48 MHz; ^{31}P: 121.49 MHz) using the solvent as the chemical shift standard, except for ^{31}P NMR, where the chemical shifts are quoted relative to 85% H_3PO_4 in D_2O. All MAS NMR experiments were performed at the National Ultrahigh-field NMR Facility for Solids (Ottawa, Canada) on a Bruker Avance II NMR spectrometer operating at 21.1 T. A double-resonance 3.2-mm Bruker probe with magic angle spinning (MAS) was used to acquire ^{1}H and ^{13}C MAS NMR spectra. ^{1}H and ^{13}C NMR chemical shifts were referenced to neat TMS using adamantane as a secondary chemical shift reference. ^{1}H MAS NMR spectra were recorded at a resonance frequency of 900.2 MHz. Samples were spun at a spinning speed of 20 kHz in 3.2-mm (o.d.) ZrO_2 rotors. A single pulse sequence with background suppression was used in ^{1}H NMR experiments with a r.f. pulse length of 2.5 μs (π/2 pulse) and a 10-s relaxation delay between pulses, which was found to be sufficient for complete relaxation. A total of 64 scans were accumulated in each ^{1}H NMR experiment. ^{13}C CP/MAS NMR spectra were recorded at a resonance frequency of 226.4 MHz at 15 kHz MAS. The CP contact time in all experiments was 1 ms, with a 5-s relaxation delay between pulses. Between 2k and 10k scans were accumulated in ^{13}C CP/MAS NMR experiments, depending on the amount of sample available. SPINAL-64 proton decoupling was employed during spectra acquisition. ^{31}P CP/MAS NMR spectra were acquired using a double-resonance 2.5 mm MAS Bruker probe at a resonance frequency of 364.4 MHz at 20 kHz MAS. The CP contact time in all experiments was 3 ms with a delay between acquisitions of 20 seconds. SPINAL-64 proton decoupling was used during spectra acquisition. Between 256 and 2048 scans were collected, depending on the amount of sample available. ^{31}P NMR chemical shifts were referenced to 85% H_3PO_4 using solid $(NH_4)H_2PO_4$ (ADP) as a secondary chemical shift reference. The same ADP sample was used to set up the ^{31}P CP/MAS conditions. All chemical shifts and coupling constants are reported in ppm and Hz, respectively. The glass transition temperature (T_g) was deter-

mined using a Perkin–Elmer 5A DSC7 equipped with a 5B TAC 7/DS thermal controller. Calibration standards were water and indium. The accuracy was ±0.1 °C and ±0.1% for Δ*Cp*. The sample weights ranged from 5 to 10 mg, and the scan rate was adjusted to 10 °C/min. TGA data were acquired with a Perkin–Elmer TGA 7 between 50 and 950 °C at a heating rate of 3 °C/min under a nitrogen atmosphere. UV/Vis spectra were recorded with a Varian Cary 50 spectrophotometer. Emission and excitation spectra were obtained by using a double monochromator Fluorolog 2 instrument from Spex. Fluorescence lifetimes were measured on a Timemaster model TM-3/2003 apparatus from PTI. The source was a nitrogen laser equipped with a high-resolution dye laser (fwhm ca. 1500 ps), and the fluorescence lifetimes were obtained from deconvolution and distribution lifetime analyses. Quantum yields were measured against $[Ru(bpy)_3](Cl)_2$ ($\Phi_e = 0.376 \pm 0.036$) in PrCN.[22]

Spin-Lattice Relaxation Times (T_1) and NOE Measurements: The T_1's were measured by the inversion recovery pulse technique. The measurements were performed with a Bruker AC-F 300 NMR spectrometer operating at 121.50 MHz for ^{31}P. The temperature was 293 K, and the sampling was done over a 20,000 Hz sweep width using 8192 data points to describe the FID. The solutions were saturated in all cases to improve the signal to-noise ratio. The uncertainties are 0.05 s based on multiple measurements (at least three). The NOE constants were measured using the inverse-gated method. On the basis of the reproducibility of the measurements, the accuracy of the method is estimated to be 10%. The internal standard (PBr_5) was inside a sealed capillary tube to avoid contact with the samples.

General Procedure for the Syntheses of diNC-Containing Polymers 4–6: DiNC (0.150 mmol), diluted in 2 mL of CH_2Cl_2, was added over 30 min to a stirred solution of the homo- or heterobimetallic precursor (0.150 mmol) in 3 mL of CH_2Cl_2. An orange solid began to precipitate within a few minutes, and the solution was stirred for 1 d. The solid was then collected by filtration, washed with Et_2O (2 × 5 mL) and CH_2Cl_2 (5 mL), and dried under vacuum.

4a: Yield 92% (182 mg). IR (KBr): $\tilde{\nu}$ = 2170 (m) (ν_{CN}), 1630 ($\nu_{C=N}$) cm^{-1}. ^1H MAS NMR: δ = 10–6.65 (m, 48 H, Ph), 3.90 (m, 4 H, PCH_2P), 3.19 (m, 4 H, OCH_2) ppm. ^{31}P MAS NMR: δ = 24.0 (m, 2 P), 14.1 (m, 2 P) ppm. $(C_{66}H_{56}Cl_2N_2O_2P_4Pd_2)_n$ (1316.8)$_n$: calcd. C 60.20, H 4.29, N 2.13; found C 59.94, H 4.33, N 2.18. UV/Vis (2-MeTHF/298 K): λ = 293, 386, 450 nm.

4b: Yield 89% (200 mg). IR (KBr): $\tilde{\nu}$ = 2177 (s) (ν_{CN}), 1634 ($\nu_{C=N}$) cm^{-1}. ^1H MAS NMR: δ = 10–6.93 (m, 48 H, Ph), 2.97 (m, 8 H, OCH_2 + PCH_2P) ppm. ^{31}P MAS NMR: δ = 29.2 (m, 4 P) ppm. $(C_{66}H_{56}I_2N_2O_2P_4Pd_2)_n$ (1499.7)$_n$: calcd. C 52.86, H 3.76, N 1.87; found C 52.68, H 3.65, N 1.80. UV/Vis (2-MeTHF/298 K): λ = 299, 376, 446 nm.

5b: Yield 87% (207 mg). IR (CH_2Cl_2): $\tilde{\nu}$ = 2173 (s) (ν_{CN}), 1625 ($\nu_{C=N}$) cm^{-1}. ^1H MAS NMR: δ = 10–7.07 (m, 48 H, Ph), 3.00 (m, 8 H, OCH_2 + PCH_2P) ppm. ^{31}P MAS NMR: δ = 22.6 (m, 4 P) ppm. $(C_{66}H_{56}I_2N_2O_2P_4PdPt)_n$ (1588.4)$_n$: calcd. C 49.91, H 3.55, N 1.76; found C 49.59, H 3.40, N 1.62. UV/Vis (2-MeTHF/298 K): λ = 303, 374, 440 nm.

6a: Yield 93% (208 mg). IR (KBr): $\tilde{\nu}$ = 2170 (m) (ν_{CN}), 1630 ($\nu_{C=N}$) cm^{-1}. ^1H MAS NMR: δ = 10.1–7.14 (m, 48 H, Ph), 3.66 (m, 8 H, PCH_2P + OCH_2) ppm. ^{31}P MAS NMR: δ = 11.9 (m, 4 P) ppm. $(C_{66}H_{56}Cl_2N_2O_2P_4Pt_2)_n$ (1494.2)$_n$: calcd. C 53.06, H 3.78, N 1.87; found C 53.58, H 3.67, N 1.74. UV/Vis (2-MeTHF/298 K): λ = 280, 360, 444nm.

6b: Yield 89% (224 mg). IR (KBr): $\tilde{\nu}$ = 2163 (s) (ν_{CN}), 1632 ($\nu_{C=N}$) cm^{-1}. ^1H NMR ([D$_6$]DMSO): δ = 8.32–6.67 (m, 48 H, Ph), 3.27 (m, 8 H, PCH_2P + OCH_2) ppm. $^{31}P\{^1H\}$ NMR ([D$_6$]DMSO): δ = 24.6 (m, $^1J_{Pt,P}$ = 3010 Hz, 4 P) ppm. $(C_{66}H_{56}I_2N_2O_2P_4Pt_2)_n$ (1677.1)$_n$: calcd. C 47.27, H 3.37, N 1.67; found C 47.03, H 3.09, N 1.78. UV/Vis (2-MeTHF/298 K): λ = 298, 364, 464 nm.

General Procedure for the Syntheses of *t*BudiNC-Containing Polymers 7–9: *t*BudiNC (0.150 mmol), diluted in 2 mL of CH_2Cl_2, was added over 30 min to a stirred solution of the homo- or heterobimetallic precursor (0.150 mmol) in 3 mL of CH_2Cl_2. The solution was stirred for another day, then the solvent was removed on a rotary evaporator in vacuo. The residue was dissolved in a minimum amount of CH_2Cl_2 and diethyl ether was slowly added. The precipitate formed was filtered, washed with Et_2O (2 × 5 mL), and dried under vacuum.

7: Yield 91% (195 mg). IR (KBr): $\tilde{\nu}$ = 2153 (m) (ν_{CN}), 1629 ($\nu_{C=N}$) cm^{-1}. ^1H NMR (CD_2Cl_2): δ = 8.38–6.72 (m, 46 H, Ph), 5.35 (br. s, 4 H, OCH_2), 3.49 (m, 4 H, PCH_2P), 1.19 (m, 18 H, CH_3) ppm. $^{31}P\{^1H\}$ NMR(CD_2Cl_2): δ = 16.7 (m, 2 P), 17.3 (m, 2 P) ppm. $^{13}C\{^1H\}$ NMR (CD_2Cl_2): δ = 166.4 (NC), 150–128 (Ph), 68.2 (OCH_2), 39.1, 32.7 [C(CH$_3$)$_3$] ppm. $(C_{74}H_{72}Cl_2N_2O_2P_4Pd_2)_n$ (1429.0)$_n$: calcd. C 62.20, H 5.08, N 1.96; found C 61.89, H 5.28, N 1.78.

8: Yield 89% (203 mg). IR (KBr): $\tilde{\nu}$ = 2164 (m) (ν_{CN}), 1625 ($\nu_{C=N}$) cm^{-1}. ^1H NMR (CD_2Cl_2): δ = 8.46–6.82 (m, 46 H, Ph), 5.33 (br. s, 4 H, OCH_2), 3.47 (m, 4 H, PCH_2P), 1.29 [s, br., 18 H, C(CH_3)$_3$] ppm. $^{31}P\{^1H\}$ NMR (CD_2Cl_2): δ = 16.4 [m, $^1J_{Pt,P}$ = 2690 Hz, 2 P, Pt-P(μ-d)], 18.7 [m, 2 P, Pd-P(μ-d)] ppm. $^{13}C\{^1H\}$ NMR (CD_2Cl_2): δ = 166.7 (NC), 150–128 (Ph), 68.9 (OCH_2), 38.4, 32.7 [C(CH$_3$)$_3$] ppm. $(C_{74}H_{72}Cl_2N_2O_2P_4PdPt)_n$ (1517.7)$_n$: calcd. C 58.56, H 4.78, N 1.85; found C 58.78, H 4.98, N 1.95.

9: Yield 92% (222 mg). IR (KBr): $\tilde{\nu}$ = 2167 (m) (ν_{CN}), 1624 ($\nu_{C=N}$) cm^{-1}. ^1H NMR (CD_2Cl_2): δ = 8.24–6.82 (m, 46 H, Ph), 5.43 (br. s, 4 H, OCH_2), 3.52 (m, 4 H, PCH_2P), 1.10 [br. s, 18 H, C(CH_3)$_3$] ppm. $^{31}P\{^1H\}$ NMR (CD_2Cl_2): δ = 0.3 (m, $^1J_{Pt,P}$ = 2550 Hz, 4 P) ppm. $^{13}C\{^1H\}$ NMR (CD_2Cl_2): δ = 166.6 (NC), 150–128 (Ph), 69.2 (OCH_2), 39.1, 32.7 [C(CH$_3$)$_3$] ppm. $(C_{74}H_{72}Cl_2N_2O_2P_4Pt_2)_n$ (1606.4)$_n$: calcd. C 55.33, H 4.52, N 1.74; found C 55.36, H 4.32, N 1.88.

[ClPd(μ-dppm)$_2$(μ-CN-C$_6$H$_4$-*i*Pr)PdCl] (10): 1-Isocyano-4-isopropylbenzene (0.100 mmol), diluted in 1 mL of CH_2Cl_2, was added over 30 min to a stirred solution of **1a** (0.100 mmol) in 3 mL of CH_2Cl_2. The solution was stirred overnight, then the solvent was removed on a rotary evaporator in vacuo. The residue was dissolved in a minimum amount of CH_2Cl_2 and hexane was slowly added. The precipitate formed was filtered, washed with Et_2O (2 × 5 mL), and dried under vacuum. Slow evaporation of **10** in CH_2Cl_2 furnished orange needles. Yield 92% (110 mg). IR (KBr): $\tilde{\nu}$ = 1633 ($\nu_{C=N}$) cm^{-1}. ^1H NMR (CD_2Cl_2): δ = 8.15–6.82 (m, 44 H, Ph), 3.83 (br. m, 4 H, PCH_2P), 2.31 [sept, $^3J_{H,H}$ = 7.4 Hz, 1 H, CH(CH$_3$)$_2$], 1.38 [d, $^3J_{H,H}$ = 7.4 Hz, 6 H, CH(CH_3)$_2$] ppm. $^{31}P\{^1H\}$ NMR (CD_2Cl_2): δ = 17.8 (s) ppm. $C_{60}H_{55}Cl_2NP_4Pd_2$ (1198.1): calcd. C 60.17, H 4.63, N 1.17; found C 60.06, H 4.49, N 1.04.

X-ray Crystallography: Single crystals of *t*BudiNC were obtained by recrystallization from hexane and were coated with perfluoroalkyl ether oil (ABCR), mounted on a glass fiber, and frozen in the cold nitrogen stream of the goniometer. The data were collected with a Stoe IPDS diffractometer. The data were reduced (Integrate in IPDS) and corrected for absorption (FACEIT in IPDS). The structure was solved by direct methods and refined by full-matrix least-squares on F^2 (SHELXTL). Single crystals of **10** were grown by slow evaporation of a solution of **10** in CH_2Cl_2 at 298 K. Data were collected with an Enraf–Nonius CAD-4 automatic dif-

fractometer using ω scans. The DIFRAC[23] program was used for centering, indexing, and data collection. Two standard reflections were measured every 200 reflections; no intensity decay was observed during data collection. The data were corrected for absorption by empirical methods based on psi scans and reduced with the NRCVAX[24] programs. They were solved using SHELXS-90[25a] and refined by full-matrix least-squares on F^2 with SHELXL-97.[25b] Non-hydrogen atoms were refined anisotropically, whereas hydrogen atoms were placed at idealized calculated geometric position and refined isotropically using a riding model. The crystal was a twin and the final absolute structure was not assigned. The final BASF parameter is 0.45(4). The absolute structure was determined by anomalous dispersion effects.[26] Crystal and refinement data for *t*BudiNC and **10** are presented in Table 3.

Table 3. Crystal and refinement data for *t*BudiNC and **10**.

	*t*BudiNC	**10**
Empirical formula	$C_{24}H_{28}N_2O_2$	$C_{60}H_{55}Cl_2NP_4Pd_2$
Formula weight	376.48	1197.63
Color	colorless	orange
Crystal size [mm]	$0.30\times0.30\times0.1$	$0.10\times0.20\times0.50$
Temperature [K]	173(2)	293(2)
Crystal system	triclinic	tetragonal
Space group	$P\bar{1}$	$P4_1$
a [Å]	12.7878(14)	21.682(4)
b [Å]	14.0209(15)	21.682(4)
c [Å]	15.1198(16)	14.1684(18)
α [°]	84.1059(19)	90
β [°]	66.6321(17)	90
γ [°]	64.7552(17)	90
Volume [Å^3]	2244(4)	6661(15)
Z	4	4
Calcd. density [Mg m^{-3}]	1.115	1.194
Scan mode	ω	ω
F(000)	808	2432
Absorption coeff. [mm^{-1}]	0.071	6.246
θ range	1.47 to 25.00°	2.04 to 69.98°
Limiting indices	$-15 \le h \le 15$	$-26 \le h \le 0$
	$-16 \le k \le 16$	$0 \le k \le 26$
	$-17 \le l \le 17$	$0 \le l \le 17$
Reflections collected	28787	6507
Independent reflections	7892	3435
Min./Max. transmission	0.9929 and 0.9790	–0.764 and 0.776
Data/restraints/parameters	7892/0/517	3435/1/582
Goodness-of-fit on F^2	1.043	0.962
Final R indices [$I > 2\sigma(I)$][a]	$R1$ = 0.0655	$R1$ = 0.0742
	$wR2$ = 0.1951	$wR2$ = 0.2014
R indices (all data)	$R1$ = 0.0896	$R1$ = 0.1552
	$wR2$ = 0.2097	$wR2$ = 0.168

[a] $R1 = \Sigma||F_o| - |F_c||/\Sigma|F_o|$; $wR2 = \{\Sigma[w(F_o^2 - F_c^2)^2]/\Sigma(F_o^4)\}^{1/2}$; weight = $1/[\sigma^2(F_o^2) + (AP)^2 + (BP)]$ where $P = [\max(F_o^2, 0) + 2F_c^2]/3$; $A = 0.0890$ and $B = 11.4580$ for *t*BudiNC, and $A = 0.1060$ and $B = 0.000$ for **10**.

CCDC-711704 (for *t*BudiNC) and -718276 (for **10**) contain the supplementary data for *t*BudiNC and **10**, respectively. These data can be obtained free of charge from the Cambridge Crystallographic Data Center via www.ccdc.cam.ac.uk/data_request/cif.

Supporting Information (see also the footnote on the first page of this article): TGA traces for *t*BudiNC-containing A-frame polymers **7**–**9**; TGA weight loss assignment for polymers **4**–**9**; MALDI-TOF spectra for A-frame heterobimetallic polymer **6a**; T_1 curves for model compound **10** and polymer **7**; emission and excitation spectra in the solid sate for *t*BudiNC, **4a**, **4b**, **5b**, **6a**, **6b**, **7**, **8**, and **9**.

Acknowledgments

P. D. H. thanks the Natural Sciences and Engineering Research Council of Canada (NSERC) and the Fonds Québécois sur la Recherche des Sciences de la Nature et des Technologies (FQRNT) for a postdoctoral fellowship for S. C., and the Center d'Études sur les Matériaux Optiques et Photoniques de l'Université de Sherbrooke (CEMOPUS) for funding. M. K. thanks the French Ministère de la Recherche et Technologie and the Centre National de la Recherche Scientifique (CNRS) for financial support and a PhD grant to S. C. Access to the 900 MHz NMR spectrometer was provided by the National Ultrahigh Field NMR Facility for Solids (Ottawa, Canada), a national research facility funded by the Canada Foundation for Innovation, the Ontario Innovation Trust, Recherche Québec, the National Research Council Canada, and Bruker BioSpin and managed by the University of Ottawa (www.nmr900.ca). The NSERC is also acknowledged for a Major Resources Support grant.

[1] For recent reviews, see: a) K. A. Williams, A. J. Boydston, C. W. Bielawski, *Chem. Soc. Rev.* **2007**, *36*, 729–744; b) W.-Y. Wong, *Dalton Trans.* **2007**, 4495–4510.

[2] a) P. D. Harvey, *Frontiers in Transition Metal-Containing Polymers*, John Wiley & Sons Inc., **2007**, pp. 321–368; b) *Macromolecules Containing Metal and Metal-Like Elements* (Eds.: A. S. Abd-El-Aziz, C. E. Carraher Jr., C. U. Pittman Jr., M. Zeldin), John Wiley & Sons, **2006**, vol. 6, pp. 1–47; c) R. D. Archer, *Inorganic and Organometallic Polymers*, John Wiley & Sons, New York, **2001**.

[3] a) N. J. Long, C. K. Williams, *Angew. Chem. Int. Ed.* **2003**, *42*, 2586–2617; b) W.-Y. J. Wong, *J. Inorg. Organomet. Polym. Mater.* **2005**, *15*, 197–219; c) W.-Y. Wong, C.-L. Ho, *Coord. Chem. Rev.* **2006**, *250*, 2627–2690; d) V. W.-W. Yam, K. M.-C. Wong, *Top. Curr. Chem.* **2005**, *257*, 1–32; e) V. W.-W. Yam, *C. R. Chim.* **2005**, *8*, 1194–1203; f) P. D. Harvey, in *Macromolecules Containing Metal and Metal-Like Elements* (Eds.: A. S. Abd-El-Aziz, C. E. Carraher Jr., C. U. Pittman Jr., M. Zeldin), John Wiley and Sons Inc., New York, **2005**, Vol. 5, pp. 83–116; g) C. G. Carson, R. A. Gerhardt, R. Tannenbaum, *J. Phys. Chem. B* **2007**, *111*, 14114–14120; h) T. Tanase, E. Goto, R. A. Begum, M. Hamaguchi, S. Zhan, M. Iida, K. Sakai, *Organometallics* **2004**, *23*, 5975–5978.

[4] a) B. E. Bursten, R. F. Fenske, *Inorg. Chem.* **1977**, *16*, 963–964; b) J. A. Howell, J. Y. Saillard, A. L. Beuze, G. Jaouen, *J. Chem. Soc., Dalton Trans.* **1982**, 2533–2537; c) R. L. White-Morris, M. Stender, D. S. Tinti, A. L. Balch, *Inorg. Chem.* **2003**, *42*, 3237–3244; d) D. Lentz, *Angew. Chem. Int. Ed. Engl.* **1994**, *33*, 1315–1331.

[5] a) M. Knorr, C. Strohmann, *Organometallics* **1999**, *18*, 248–257; b) M. Knorr, I. Jourdain, G. Crini, K. Frank, H. Sachdev, C. Strohmann, *Eur. J. Inorg. Chem.* **2002**, 2419–2426; c) M. Knorr, I. Jourdain, D. Lentz, S. Willemsen, C. Strohmann, *J. Organomet. Chem.* **2003**, *684*, 216–229; d) Y. Yamamoto, H. Yamazaki, *Inorg. Chem.* **1986**, *25*, 3327–3329; e) M. L. Kuznetsov, M. L. Pombeiro, *Dalton Trans.* **2003**, 738–747.

[6] a) A. Guitard, A. Mari, A. L. Beauchamp, Y. Dartiguenave, M. Dartiguenave, *Inorg. Chem.* **1983**, *22*, 1603–1606; b) S. J. Milder, R. A. Goldbeck, D. S. Kliger, H. B. Gray, *J. Am. Chem. Soc.* **1980**, *102*, 6761–6764 and references cited therein; c) A. Efraty, I. Feinstein, L. Wakerle, F. Frolow, *Angew. Chem. Int. Ed. Engl.* **1980**, *19*, 633–634; d) S. Schröllkamp, W. Sperber, D. Lentz, W. P. Fehlhammer, *Chem. Ber.* **1994**, *127*, 621–629; e) S. Coco, E. Espinet, P. Espinet, I. Palape, *Dalton Trans.* **2007**,

3267–3272; f) O. Elbjeirami, M. W. A. Gonser, B. N. Stewart, A. E. Bruce, M. R. M. Bruce, T. R. Cundari, M. A. Omary, *Dalton Trans.* **2009**, 1522–1533.

[7] a) J.-F. Bérubé, K. Gagnon, D. Fortin, A. Decken, P. D. Harvey, *Inorg. Chem.* **2006**, *45*, 2812–2823; b) S. Sicard, J.-F. Bérubé, D. Samar, A. Messaoudi, D. Fortin, F. Lebrun, J.-F. Fortin, A. Decken, P. D. Harvey, *Inorg. Chem.* **2004**, *43*, 5321–5334; c) S. Clément, S. Mohammed, K. Gagnon, D. Fortin, A. Abd-El-Aziz, M. Knorr, P. D. Harvey, *J. Inorg. Organomet. Polym. Mater.* **2008**, *18*, 104–110.

[8] R. J. Angelici, M. H. Quick, G. A. Kraus, D. T. Plummer, *Inorg. Chem.* **1982**, *21*, 2178–2184.

[9] M. A. Khan, A. J. McAlees, *Inorg. Chim. Acta* **1985**, *104*, 109–114.

[10] a) D. Evrard, S. Clément, D. Lucas, B. Hanquet, M. Knorr, C. Strohmann, A. Decken, Y. Mugnier, P. D. Harvey, *Inorg. Chem.* **2006**, *45*, 1305–1315; b) S. Clément, S. M. Aly, D. Bellows, D. Fortin, C. Strohmann, L. Guyard, A. S. Abd-El-Aziz, M. Knorr, P. D. Harvey, *Inorg. Chem.*, DOI: 10.1021/ic8023315.

[11] D. Samar, J.-F. Fortin, D. Fortin, A. Decken, P. D. Harvey, *J. Inorg. Organomet. Polym. Mater.* **2006**, *15*, 411–429.

[12] M. Turcotte, P. D. Harvey, *Inorg. Chem.* **2002**, *41*, 2971–2974.

[13] T_1 decreases with the field (H_0), thus indicating the extreme narrowing limit.

[14] a) R. S. Drago, *Physical Methods for Chemists*, 2nd ed., Saunders College Publishers, New York **1992**; b) F. W. Wehrli, T. Wirthlin, *Interpretation of Carbon-13 NMR Spectra*, Heyden, London, **1980**.

[15] a) J. L. Marshall, M. D. Hopkins, V. M. Miskowski, H. B. Gray, *Inorg. Chem.* **1992**, *31*, 5034–5040; b) C. M. Che, V. W.-W. Yam, W.-T. Wong, T. F. Lai, *Inorg. Chem.* **1989**, *28*, 2908–2910.

[16] N. Turro, *Modern Molecular Photochemistry*, University Science Books, Sausalito, CA, **1991**.

[17] H. A. Nieuwenhius, D. J. Stufkens, A. Vicek Jr., *Inorg. Chem.* **1995**, *34*, 3879–3886.

[18] S. Clement, S. M. Aly, D. Fortin, L. Guyard, M. Knorr, A. Abd-El-Aziz, P. D. Harvey, *Inorg. Chem.* **2008**, *47*, 10816–10824.

[19] P. G. Pringle, B. L. Shaw, *J. Chem. Soc., Dalton Trans.* **1983**, *5*, 889–897.

[20] M. C. Grossel, J. R. Batson, R. P. Moulding, K. R. Seddon, *J. Organomet. Chem.* **1986**, *304*, 391–423.

[21] W. P. Weber, G. W. Gokel, *Tetrahedron Lett.* **1972**, *13*, 1637–1640.

[22] J. N. Demas, G. A. Crosby, *J. Am. Chem. Soc.* **1971**, *93*, 2841–2847.

[23] H. D. Flack, E. Blanc, D. Schwarzenbach, *J. Appl. Crystallogr.* **1992**, *25*, 455–459.

[24] E. J. Gabe, Y. Le Page, J.-P. Charland, F. L. Lee, P. S. White, *J. Appl. Crystallogr.* **1989**, *22*, 384–387.

[25] a) G. M. Sheldrick, *SHELXS-90*, University of Göttingen, Germany, **1990**; b) G. M. Sheldrick, *SHELXL97*, University of Göttingen, Germany, **1997**.

[26] H. D. Flack, *Acta Crystallogr., Sect. A* **1983**, *39*, 876–881.

Received: January 29, 2009
Published Online: May 4, 2009

